Table 1. Worldwide (Ww) and New York City (NYC) depositions of ^{90}Sr. The average ratio was 0.15. The 1966 figures are estimates.

Year	Ww (Mc)	NYC (mc/km^2)	Ratio (Ww : NYC)
1954	0.35	2.76	0.13
1955	.60	3.57	.17
1956	.55	4.43	.12
1957	.50	4.44	.11
1958	.90	6.16	.15
1959	1.13	8.68	.13
1960	0.38	1.58	.24
1961	.46	2.43	.19
1962	1.53	11.07	.14
1963	2.59	23.87	.11
1964	1.84	15.85	.12
1965	1.00	5.53	.18
1966	0.4	2.3	.17

ing the highest frequency. Plus values occur at least once during all months but September, October, and November; in every year, March, April, and May were all plus. These observations indicate that in New York City the peak is indeed a spring phenomenon generally centered on and most intense in the month of April. Conversely, the fallout is lowest in the autumn, with September having the highest frequency of minimum values.

Predictions of ^{90}Sr deposition in New York City are important, particularly in estimation of future human-body burdens (*12*). The method of predicting ^{90}Sr fallout there is based on predictions of worldwide deposition and the observed relation between worldwide and New York City fallout (*5*). Since the beginning of the current ban, the stratospheric inventory of ^{90}Sr has been decreasing, with an apparent half-residence time of about 10 months (*2*). Extrapolation of the measured stratospheric burdens yields the inventory decrease for any year, which equals the expected global fallout for that year, less the change in tropospheric inventory. Then, on the assumption that the ratio of worldwide to New York fallout is constant (Table 1), the deposition value for New York City can be calculated. This constant for ^{90}Sr is 6.6 mc/km^2 in New York for every megacurie of worldwide fallout. By this method yearly predictions of ^{90}Sr fallout from 1966 through 1970 are respectively 2.3, 1.1, 0.48, 0.21, and 0.09 mc/km^2.

Table 2. Stratospheric half-residence time (HRT) derived from fallout data for New York City. Figures for 1966 are partially estimated.

Period	Fallout (mc/km^2)	HRT (months)
	First moratorium	
Dec. 58–Nov. 59	9.16	5
Dec. 59–Nov. 60	1.74	
May 59–Apr. 60	3.93	9
May 60–Apr. 61	1.56	
	Current test ban	
Jan. 63–Dec. 63	23.87	20
Jan. 64–Dec. 64	15.85	8
Jan. 65–Dec. 65	5.53	10
Jan. 66–Dec. 66	2.3	
June 63–May 64	22.22	9
June 64–May 65	9.02	9
June 65–May 66	3.71	

During the course of the year (*7*) alternate predictions of yearly and monthly fallouts are computed; the historical record of ^{90}Sr fallout in New York City is employed, by use of the monthly values relative to the yearly deposition. For example, the cumulative deposition to the end of June 1966 was 1.71 mc/km^2. On the average, 67.6 percent of the annual deposition occurs by July 1; thus 2.5 mc/km^2 is predicted for the year. This is in good agreement with the original prediction based upon stratospheric depletion.

In summary: By the middle of 1966 the peak of accumulated ^{90}Sr on Earth's surface near New York passed; the deposit is now decaying faster than new material is falling. The stratospheric half-residence time of 8 to 10 months, based on the rate of ^{90}Sr deposition in New York, is in very good agreement with estimates from direct measurements.

The overpowering variations in the absolute deposition levels were virtually eliminated by a method of normalizing the monthly data on fallout on a continuing basis; thus seasonal oscillation in fallout is easily observable. This spring peak is extremely symmetrical and constant relative to the rest of the year; it is independent of the timing and magnitude of atmospheric tests.

Predictions of fallout in New York, based on empirical observations and on the assumption of no substantial additions of ^{90}Sr to the atmosphere, indicate that less than 0.1 mc/km^2 will be deposited during 1970—less than 1 percent of deposition during the peak year, 1963.

H. L. Volchok
Health and Safety Laboratory, U.S. Atomic Energy Commission, New York

References and Notes

1. One of 160 stations in the AEC network.
2. Calculated from direct measurements: H. W. Feely and P. E. Biscaye, *41st Monthly Report on Project Stardust* (U.S. Dept. of Defense Atomic Support Agency, 1965).
3. G. A. Welford and J. H. Harley, *Health and Safety Lab. Rept. HASL-42* (1958); *Science* **131**, 3416 (1960).
4. H. L. Volchok, *Health and Safety Lab. Rept. HASL-174* (1966).
5. ———, *Science* **145**, 3639 (1964).
6. L. D. Y. Ong and F. Y. Durkan, *Health and Safety Lab. Rept. HASL-158* (1965).
7. H. L. Volchok, *Health and Safety Lab. Rept. HASL-155* (1965); *Rept. HASL-172* (1966).
8. L. T. Alexander *et al., AEC Report. TID-6567* (1961); E. P. Hardy *et al., AEC Report TID-17090* (1962); E. P. Hardy and J. Rivera, *Health and Safety Lab. Rept. HASL-149* (1964).
9. E. P. Hardy and J. Rivera, in *Health and Safety Lab. Rept. HASL-173* (1966).
10. M. W. Meyer, V. T. Velassis, J. S. Allen, *Health and Safety Lab. Rept. HASL-171* (1966).
11. N. G. Stewart, R. N. Crooks, E. M. R. Fisher, *Atomic Energy Research Establishment Report HPR 2017* (1956); L. B. Lockhart, Jr., A. W. Paterson, Jr., A. W. Saunders, Jr., R. W. Black, *Naval Res. Lab. Rept. 5528* (1960); P. W. Krey and W. C. Rosa, Jr., *HASL Surface Air Sampling Program Nov. 1964* (1965).
12. J. Rivera, in *Health and Safety Lab. Rept. HASL-173* (1966).

27 January 1967; revised 12 April 1967

Jupiter's Atmosphere: Its Structure and Composition

Abstract. *Recent laboratory and observational data support the hypothesis that the composition of Jupiter's atmosphere is consistent with the relative abundances of the elements found in the sun. A model based on this assumption provides a reasonable interpretation of abundances of hydrogen and other gases obtained from studies of various regions of the planet's spectrum. Two presently unidentified absorptions may be caused by organic molecules in the Jovian atmosphere.*

The composition of Jupiter's atmosphere remains an enigma, despite the fact that direct measurement of the hydrogen abundance has been possible for several years (*1*), while two minor constituents, methane and ammonia, were identified long ago (*2*). Determinations of the amount of hydrogen, made by various workers from observations of the quadrupole absorptions in the infrared, differ widely among themselves. The best new values also appear to conflict with independent H_2 abundance determinations from analysis of the ultraviolet reflectivity of the planet. Deductions concerning other possible constituents are strongly dependent on the resolution of these dilemmas; as yet no additional gases have been discovered (*3*). This report discusses some preliminary results of our efforts at reevaluating these problems. Our study is based on a structural model for the Jovian atmosphere that appears to be consistent

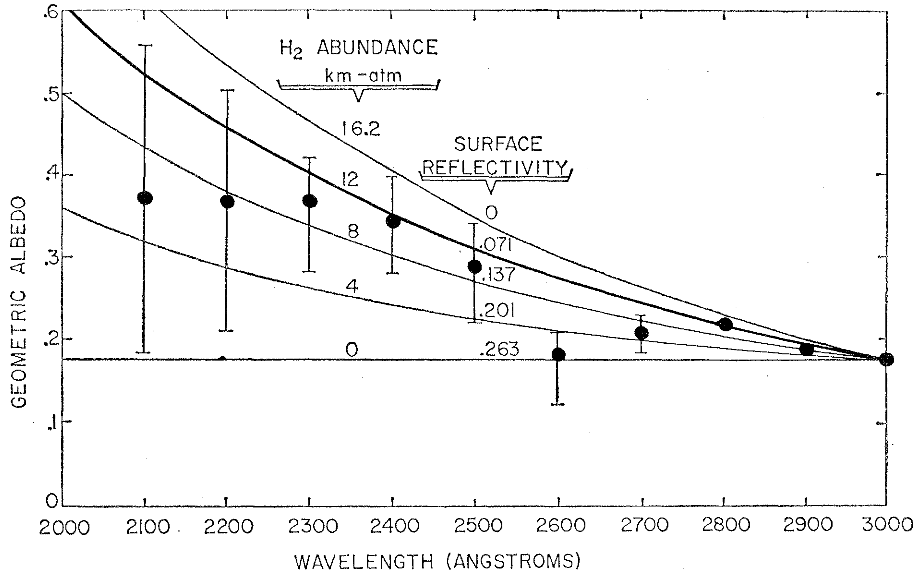

Fig. 1. Ultraviolet geometric albedo for several H_2 abundance–surface reflectivity combinations matching the observed Jovian albedo at 3000 Å.

with available observations. To provide a model for the chemical composition, we have started with the hypothesis that the elements are present in solar abundances, as suggested by the following argument.

The recent work of Rank, Fink, and Wiggins (*4*) offers the best currently available values for the H_2 abundance as derived from the quadrupole absorptions; an average value of 240 km-atm is obtained from their determinations. Correcting this by a factor of 2 for the effective air mass, we obtain a value of 120 km-atm for the Jovian H_2 (*5*). Although there is still a large amount of uncertainty (± 50 percent) in this number, owing to the scatter in the equivalent width data, it is the best value currently available. The observed Jovian methane abundance is 150 m-atm (*6*). If one assumes that all of the carbon in Jupiter's atmosphere is present as methane, an atmospheric C/H ratio of 0.63×10^{-3} is obtained. The C/H ratio in the solar atmosphere (0.52×10^{-3}) is in good agreement with this value, considering the uncertainties involved. On the strength of this agreement, we have assumed that all the elements are present in solar abundances, but in the form of fully reduced compounds. This assumption gains support from its successful adoption in recent work on the planet's interior (*7*). Furthermore, helium must be included in relative solar concentration in order to increase the mean molecular weight to 2.3, a value within the range determined from the observation of a stellar occultation (*8*).

Table 1. Chemical equilibrium concentrations at 298°K for a model Jovian atmosphere based on solar abundances.

Reactant*	Assumed initial abundance (m-atm)	Calculated equilibrium abundances (m-atm)
H_2	120.0×10^3	120.0×10^3
He	23.5×10^3	23.5×10^3
Ne	28.5	28.5
C†	126.0	0
O_2	109.5	0
N_2	11.5	0
Si†	7.6	0
Mg†	6.0	0
S†	4.8	0
Fe†	0.89	0
CH_4	0	126.0
NH_3	0	23.0
SiH_4	0	0
SiO_2†	0	7.6
MgO†	0	6.0
H_2O	0	197.8
H_2S	0	3.91
FeS†	0	0.89

*Numerous other compounds were considered in this study but were not formed in significant amounts. †Indicates solid at 298°K.

Considering only elements with the abundance of iron or greater, one obtains the composition given in the second column of Table 1 (*9*). In order for this compositional model to represent a physically meaningful situation, the mixture must be chemically stable. We have determined the conditions of chemical equilibrium (*10*) for an appropriate group of reactants, using the solar compositional model for the initial conditions. The results showed that the second column in Table 1 does not in fact represent an equilibrium mixture; SiH_4 is unstable in the presence of water, becoming SiO_2 despite the large excess of hydrogen. The abundance of H_2S is reduced because, at these temperatures, the iron combines with sulfur to form FeS [a result pointed out by Urey several years ago (*11*)]. Since the solar abundance of sulfur is considerably higher than that of iron, however, a large amount of H_2S remains. The revised atmospheric composition is presented in the third column of Table 1, and forms a basis for comparison with the results of observations. The ultraviolet region of the spectrum will be considered first.

The ultraviolet geometric albedo for Jupiter was calculated by solving the equation of radiative transfer for a simplified Jovian model atmosphere. The model is comprised of one scattering gas (which does not absorb) distributed in hydrostatic equilibrium above an opaque Lambert surface (reference level) of reflectivity $A(\lambda)$, and of an arbitrary number of gaseous absorbers (nonscattering) which are either mixed or in diffusive equilibrium with the scatterer. Since H_2 is more than five times as abundant as He (solar composition), and scatters ten times more effectively, the one scatterer approximation should be valid to within a few percent. Isothermalcy is also assumed. With these assumptions, the geometric albedo $\bar{p}(\lambda)$ can be expressed (at opposition) as

$$\bar{p} = \pi\tau_s \int_0^1 E_3[\tau_s u + \sum_a \tau_a u^{M_a}]\,du + 2A\,E_4[L]$$

where

$$L(\lambda) = [\tau_s + \sum_a \tau_a]$$

in which

$$\tau_s(\lambda) = 2\sigma_s \frac{\Phi_o}{4\pi} n_o X_s^{\circ}$$

is the scatterer optical thickness and $\tau_a(\lambda) = 2k_a X_a^{\circ}$ is the absorber optical thickness; $\sigma_s(\lambda)$ is the Rayleigh scattering cross section per molecule, Φ_o is the Rayleigh phase function for backscattering, n_o is Loschmidt's number, $k_a(\lambda)$ is the gaseous absorption coefficient, X_s° and X_a° are the scatterer and absorber abundances, respectively, above the reference level, and $E_3[\,]$ and $E_4[\,]$ are exponential integrals. In the above definitions, λ indicates wavelength-dependent quantities. The summation is taken over the individual absorbing constituents; $M_a = 1$ if the absorber is mixed with the scatterer, while $M_a = m_a/\bar{m}$ if it is distributed in diffusive equilibrium. Here m_a is the absorber molecular weight and $\bar{m}$ is the mean molecular weight of the atmosphere.

If all absorbers are mixed with the scatterer, the expression for the albedo reduces to

$$\bar{p} = \left[\frac{\pi}{3}\frac{\tau_s}{L} + (2A - \frac{\pi\tau_s}{L} E_4\,[L])\right]$$

The observational data used in this study consist of spectra (2000 to 3000 Å) of Jupiter obtained from rockets by Stecher (*12*) and subsequently confirmed (above 2300 Å) by Evans (*13*). Stecher analyzed his observations in terms of simple Rayleigh scattering by molecular hydrogen (*12*), and obtained a best fit with the data for an H_2 abundance of 10.2 km-atm and zero surface reflectivity.

In order to confirm Stecher's results, we recalculated the albedo, using the formulation given above and requiring exact agreement with the observations at 3000 Å where no absorption is expected. Under these conditions, we obtain a best fit with the data for 12 km-atm of H_2 and 7 percent surface reflectivity. This fit is made directly to Stecher's data points and essentially confirms his conclusions. Results for abundance-reflectivity combinations giving exact agreement at 3000 Å are illustrated in Fig. 1. The maximum H_2 abundance allowed in the absence of absorption at 3000 Å is 16 km-atm, as determined for zero reflectivity, while a lower abundance limit of about 6 km-atm exists within the reported error limits.

The "best fit" curve in Fig. 1 (heavy line) suggests the presence of three absorption features previously pointed out and discussed by Stecher. These are the dip from 2400 to 2800 Å centered near 2600 Å, the gradual dropoff below 2400 Å, and the absence of measurable reflectivity below about 2100 Å (Stechers' instrument could have recorded radiation below this wavelength if the intensity were high enough). Our formulation for the albedo, in addition to permitting confirmation of Stecher's results, now puts us in a position to identify and determine abundances of the atmospheric constituents responsible for these absorptions.

Of the atmospheric constituents expected to be present on the basis of solar abundance considerations (see Table 1), only NH_3 and H_2S are important absorbers in the region 2000 to 3000 Å. Figure 2 shows the results of albedo calculations (*14*) for a range of abundances of NH_3 mixed with the atmosphere above the reference level (reflectivity = 7 percent) defined by 12 km-atm of H_2. An abundance of 230 cm-atm of NH_3 would be expected, assuming solar composition and no change in composition with height. This result is completely incompatible with the observations. Although none of the calculated curves fit the data well in the region below 2400 Å, an upper limit to the NH_3 abundance of only 0.007 cm-atm can be set by assuming that NH_3 is the only absorber and by accepting Stecher's data points without the associated error. Within the error limits, abundances up to 0.03 cm-atm of NH_3 are permitted. It is worth pointing out here that in Stecher's (*15*) original presentation of these observations, he gave a much lower value for the albedo at 2100 Å. The earlier data show much better agreement with the calculated albedo curves for ammonia absorption and suggest an abundance of ~0.05 cm-atm of NH_3 mixed with the atmosphere.

The results of a similar treatment for H_2S are shown in Fig. 3. The solar abundance prediction, as in the case for NH_3, is more than three orders of magnitude above the upper limit determined from the calculations.

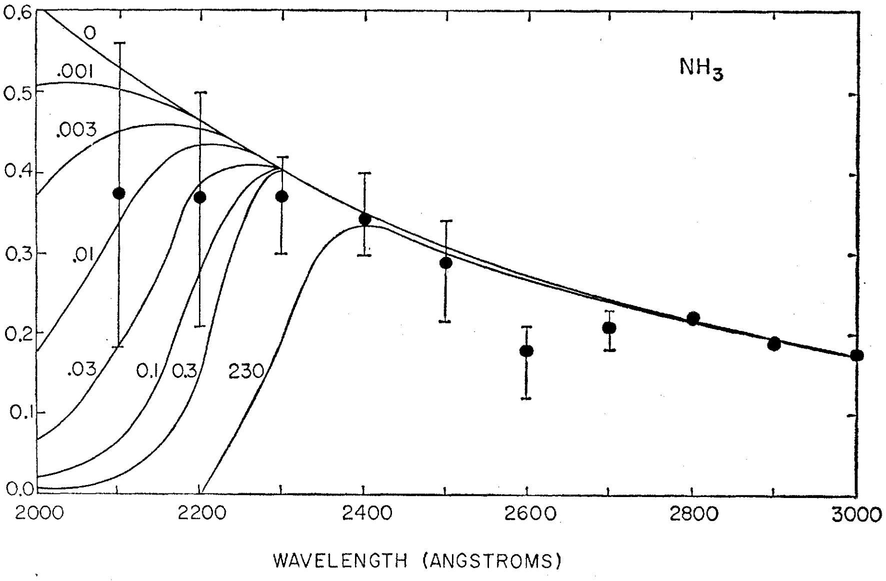

Fig. 2. Ultraviolet geometric albedo for 12-km-atm of H_2, 7 percent surface reflectivity, and various amounts of NH_3 (in cm-atm) mixed with the H_2.

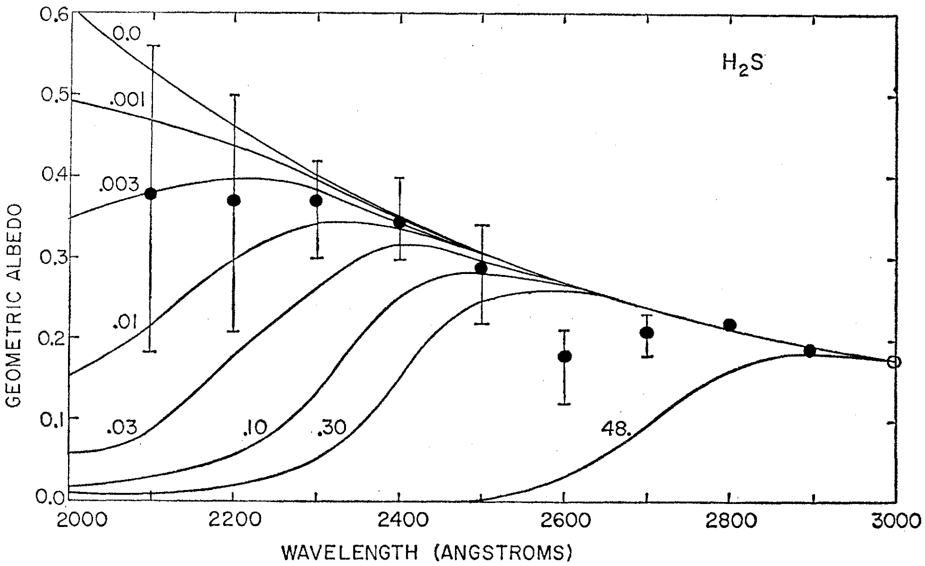

Fig. 3. Ultraviolet geometric albedo for 12 km-atm of H_2, 7 percent surface reflectivity, and various amounts of H_2S (in cm-atm) mixed with the H_2.

The upper limit to the H_2S abundance is 0.003 cm-atm for the best fit with the data points; it can be increased to 0.02 cm-atm within the error of the observations. While the H_2S profiles show a better fit to Stecher's current data (*12*) than the NH_3 profiles, the opposite is true if the original data (*15*) are used. The quality of the data prevents a better definition of the relative abundance of the two gases. This problem will remain unresolved until better spectra are obtained showing the NH_3 band structure and defining the profile with greater certainty.

To summarize, we find that (i) either NH_3 or H_2S (or a combination of the two) can account for the absorption between 2100 and 2400 Å, (ii) the abundances of these gases permitted by the observations are orders of magnitude below the solar abundance predictions, and (iii) neither gas can account for the absorption feature near 2600 Å or the absence of measurable reflectivity below 2100 Å (*16*).

We now find ourselves in the position of having contradicted our original solar-abundance hypothesis. In the case of ammonia, this dilemma can be resolved by considering the temperature profile in the atmosphere of Jupiter. Wildt (*2*) pointed out many years ago that the cloud deck observed on Jupiter is probably composed of condensed ammonia. An upper limit for the ammonia abundance at any level in the atmosphere is thus set by the ammonia vapor pressure corresponding to the temperature of that level. A comparable restriction on the hydrogen abundance can be obtained from the recent work of Trafton (*17*), who has shown that hydrogen can produce a greenhouse effect in the atmosphere of Jupiter. The atmosphere thus assumes a temperature gradient dependent on the amount of hydrogen above a given level. We have gone one step further and added an isothermal stratosphere (*18*) in radiative equilibrium with the lower atmosphere (Fig. 4).

We can now use this model to determine upper limits on the density gradient of ammonia. Ammonia temperature-density profiles for three values of the saturation coefficient σ ($\sigma = 1$ represents 100 percent relative humidity) are shown in Fig. 4. Inspection of the figure indicates that for a saturated atmosphere [the usual assumption following Kuiper (*6*)], the amount of ammonia expected above the reference level corresponding to the ultraviolet observations is only 0.006 cm-atm. This is in excellent agreement with the maximum amount permissible on the basis of the ultraviolet data (0.007 cm-atm).

The problem of the H_2S abundance is not so simple. If we adopt the temperature-density profile of Fig. 4, it is not completely certain that this gas would condense. Wildt (*19*) has suggested that H_2S would not be stable because it would be rapidly disintegrated by hydrogen atoms, leading to the precipitation of solid sulfur. It may be, of course, that Jupiter is deficient in sulfur compared with the sun, but this conclusion is presently premature. It would be extremely interesting if this turned out to be the case, however, since the abundance ratio Fe/S is greater than 1 in both the earth's crust and in meteorites (see *9*).

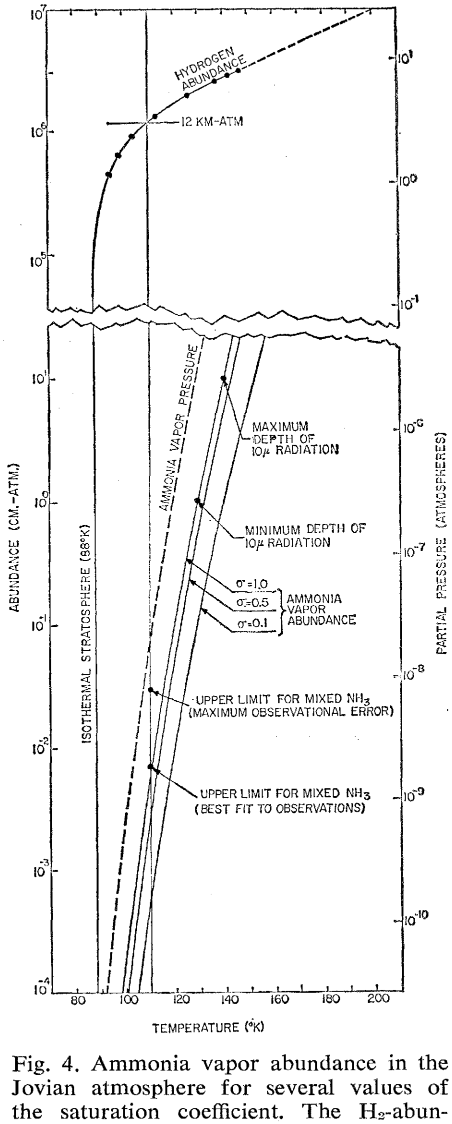

Fig. 4. Ammonia vapor abundance in the Jovian atmosphere for several values of the saturation coefficient. The H_2-abundance profile is taken from Trafton (*17*).

We still have to account for the absorption feature at 2600 Å and the absence of measurable reflectivity below 2100 Å. As an alternative to H_2S, Stecher (*12*) suggested that the forbidden photodissociation of hydrogen might lead to an absorption near 2600 Å. We have investigated this possibility and found that absorption near 2610 Å could result from forbidden transitions from the fourth vibrational level of the ground state ($X^1\Sigma_g{}^+$) to the overlying repulsive triplet state ($b^3\Sigma_u{}^+$). At the temperature of Jupiter's atmosphere, however, the population of the fourth vibrational level is down many orders of magnitude compared with the zero level. Using the H_2 absorption coefficient derived by Stecher (and confirmed in our work) for the 2600 Å feature, one would predict an extremely strong absorption from the zero level, and even the transition from the third vibrational level could easily be observed in the laboratory, contrary to experience. It thus appears that H_2 is also an unlikely candidate.

We have examined a long list of other molecules. It appears improbable that a diatomic molecule could be responsible, the only possibility being CS, which is unlikely to be present. Triatomic molecules such as HCN, PH_3, CH_2, and so forth, and the higher hydrocarbons C_2H_2, C_2H_4, C_2H_6 were also considered, again with no success. Contamination by terrestrial ozone was also rejected as a possible explanation. If we restrict ourselves to the relatively abundant elements in the Jovian atmosphere, we find that only rather complex molecules produce strong absorptions in this region. The richest source of such molecules is found from a consideration of carbon chemistry, which suggests benzene as an obvious example (*20*). We have examined this possibility rather carefully. Benzene exhibits both an absorption feature at 2600 Å and a sharp absorption increase at 2100 Å, but a detailed fit of the absorption profile to the observations does not provide a very convincing match. The amount of gas needed (0.04 cm-atm) is also rather high considering the low vapor pressure of benzene at the relevant temperatures. (Benzene crystals would have a very similar spectrum to that of the vapor, however.) It is interesting that several aromatic hydrocarbons exhibit both a weak dip at 2600 Å and a strong absorption edge at 2100 Å;

unfortunately there is no a priori way of distinguishing among these molecules. Again, the great current need is for observations at higher resolution in order that the fine structure of the 2600-Å feature becomes available for analysis. The implication that some complex molecule must be responsible is of very great interest since its identification may lead to an understanding of the colors observed in the cloud layer and could provide a firm basis for assessing the possible biological importance of Jupiter.

We may now ask whether this general picture is in agreement with observations made at other wavelengths. The temperature of 129°K determined from observations in the 10-μ region (*21*) is consistent with the presence of saturated ammonia above the clouds, as Kuiper (*6*) has pointed out. A qualitative explanation of the observed limb darkening at these wavelengths is also afforded by this model. Since the 10-μ ammonia bands are saturated, the increased air mass toward the limb will lead to lower measured temperatures because the emitting layer will be at a higher altitude. The observed ΔT of 3° to 5°K is in fair agreement with a prediction of ~3°K from Fig. 4 (for $\sec z = 2$).

The hydrogen and methane abundances we have accepted as our standards (see Table 1) were determined in the red and near infrared (0.6 to 0.9 μ). Ammonia has also been observed in this region, leading to a derivation of 7 to 10 m-atm for the mean abundance. Thus we are obviously "seeing" to deeper levels in the atmosphere at these wavelengths than in the ultraviolet, but while the hydrogen abundance has increased by only an order of magnitude, that of ammonia is more than 10^4 times greater than the amount derived from the ultraviolet observations. The difference is due to the fact that the ammonia abundance is following the saturation vapor curve, while the density of the hydrogen is increasing hydrostatically, as is evident from Fig. 4.

For this region of the spectrum, it is not possible to clearly define an atmospheric level corresponding to a given amount of gas because of the presence of the clouds. The scattering due to the cloud particles will complicate the process of line formation, rendering the determination of abundances rather uncertain. Experience with the spectrum of Venus (*22*) (which exhibits a similar behavior) strongly suggests that in the hydrogen absorption lines, the incoming radiation penetrates to lower levels than in the adjacent continuum, that is, the hydrogen abundance determination probably corresponds to an optical path extending well into the cloud layer. In addition, the condensation of ammonia must be considered when attempts are made to compare the hydrogen and ammonia abundances.

In this kind of atmosphere, absorption bands of moderate strength such as occur in the 1.0- to 2.5-μ region will correspond to much smaller amounts of gas than the very weak bands we have just discussed. Thus it is not surprising that investigators (*23*) studying this part of the spectrum derive much lower abundances for the various constituents we have mentioned.

To summarize these results, we would say that there appears to be no inconsistency between the ultraviolet and infrared observations. The differences in derived values of abundances (most notably that of hydrogen) simply correspond to different levels of penetration (or effective optical paths) into the atmosphere. This means that precise determinations of abundance ratios must be made with lines of similar intensity in the same region of the spectrum, while absolute abundances have relatively little meaning. It is clear, however, that a more detailed model atmosphere encompassing the region of the clouds and taking account of the internal heat source which now seems definitely present (*24*) must be developed to explain all of the observations in detail. The identification of the agent(s) responsible for the absorption at 2600 Å and below 2100 Å remains a mystery, although some kind of aromatic hydrocarbon seems to be the most probable absorber.

With the possible exception of the H_2S abundance, we have found no disagreement with our assumption that the composition of Jupiter's atmosphere is basically similar to that of the sun. It has not proved possible to critically test this assumption with available data, however, and additional observations are highly desirable.

With the imminent availability of spacecraft capable of missions to Jupiter, it is refreshing to discover that the planet grows simultaneously more interesting and more mysterious as it is subjected to additional investigation. It has often been postulated that the atmosphere of Jupiter represents (in composition) the matter from which the solar system was formed. The apparent similarity we have pointed out here between the atmospheres of Jupiter and the sun supports this view. The additional possibility that complex organic molecules are forming in this "primitive" environment has profound implications for studies of the origin of life on earth. It seems reasonable to conclude that missions to Jupiter promise to be among the most rewarding efforts of the space program.

JACK A. GREENSPAN
TOBIAS OWEN

Astro Sciences Center,
IIT Research Institute,
Chicago, Illinois 60616

References and Notes

1. F. R. Zabriskie, *Astron. J.* **67**, 168 (1962).
2. R. Wildt, *Veröffentl. Sternw. Göttingen* **2**, No. 22, 171 (1932).
3. T. C. Owens, *Astrophys. J.* **142**, 782 (1965); V. I. Moroz, *Astron. Zh.* **43**, 597 (1966).
4. D. H. Rank, U. Fink, T. A. Wiggins, *Astrophys. J.* **143**, 980 (1966).
5. The effective air mass is simply the equivalent optical path in the planet's atmosphere traversed by the radiation forming the spectrum in units of a single radial traversal. In the case of Jupiter, there appears to be little if any enhancement of absorption toward the edge of the disk, hence a value of 2 (a simple in and out path) seems appropriate. The abundances are measured in km-atm where 1 km-atm = 2.69×10^{24} molecules/cm^2 (standard temperature and pressure), 1 m-atm = 2.69×10^{21} molecules/cm^2, and so forth.
6. G. P. Kuiper, in *Atmospheres of the Earth and Planets*, G. P. Kuiper, Ed. (Univ. of Chicago Press, Chicago, 1952), p. 306.
7. P. J. Peebles, *Astrophys. J.* **140**, 328 (1964).
8. W. A. Baum and A. D. Code, *Astron. J.* **58**, 108 (1953). If we add sufficient helium to bring the molecular weight up to the preferred value of 3.3 given by Baum and Code, we must assume that a large amount of the original hydrogen was lost. In this case, it is difficult to see how the C/H ratio can be as small as it is, unless a large amount of carbon is tied up in some other compound. The chemical equilibrium calculations (mentioned later in our paper) suggest that no other carbon compound is likely to form in any significant abundance. Since Baum and Code actually determined the scale height rather than the molecular weight, a more reasonable way of achieving a better fit with their data would seem to be the hypothesis that the local temperature was lower than their assumed value (86°K).
9. L. H. Aller, *The Abundance of the Elements* (Interscience, New York, 1961); S. Biswas and C. E. Fichtel, *Space Sci. Rev.* **4**, 709 (1965).
10. R. Snow, *IIT Research Institute Report C929-3*, Chicago (1963). We thank Dr. Snow for many helpful discussions regarding the use of this program for our particular purposes.
11. H. C. Urey, *Geochim. Cosmochim. Acta* **1**, 209 (1951).
12. T. P. Stecher, *Astrophys. J.* **142**, 1186 (1965). Stecher also considered the effects of Rayleigh scattering by helium in Jupiter's atmosphere. Those results, however, are not of interest here.
13. D. C. Evans, *Goddard Space Flight Center Report X-613-66-172* (1966); ———, A. Boggess III, R. Scolnik, *Astron. J.* **70**, 321 (1965).

14. These calculations were performed with NH_3 absorption coefficients given by B. A. Thompson, P. Harteck, and R. R. Reeves, Jr. [*J. Geophys. Res.* **68**, 6431 (1963)]; H_2S absorption coefficients given by J. O. Sullivan and A. C. Holland [*NASA Contractor Rep. 371*, 150 (1966)]; and H_2 scattering cross sections from A. Dalgarno and D. A. Williams [*Astrophys. J.* **136**, 690 (1962)]. The NH_3 and H_2S data were degraded to a resolution of 70 Å to correspond to the observational data.
15. T. P. Stecher, *Ann. Astrophys.* **28**, 788 (1965).
16. For reasonable NH_3 abundances, the calculated albedo increases rapidly below 2000 Å. This increase continues with decreasing wavelength down to about 1450 Å. Below this wavelength the albedo again decreases.
17. L. Trafton, *Astrophys. J.* **140**, 1340 (1964). We thank R. Danielson for calling our attention to the efficacy of this approach in interpreting the atmospheric structure. Danielson and Savage (in preparation) have carried this type of analysis much further, but their purposes differ somewhat from ours.
18. An isothermal stratosphere compatible with Trafton's greenhouse model must have a temperature below 95°K. We have assumed an effective temperature of 105°K for the upper atmosphere of Jupiter [D. Taylor, *Icarus* **4**, 362 (1965)] and derived an isothermal stratospheric temperature of 88°K.
19. R. Wildt, *Astrophys. J.* **86**, 321 (1937).
20. We thank Professor G. Herzberg for a discussion of the identification problem which emphasized this possibility.
21. R. L. Wildey, B. C. Murray, J. A. Westphal, *J. Geophys. Res.* **70**, 3711 (1966).
22. J. W. Chamberlain, *Astrophys. J.* **141**, 1184 (1965).
23. G. P. Kuiper, *Mem. Soc. Roy. Sci. Liege*, **9**, 365 (1964); V. I. Moroz, *Astron. Zh.* **43**, 579 (1966); R. E. Danielson, *Astrophys. J.* **143**, 949 (1966).
24. F. Low, *Lowell Observatory Bull. No. 128*, **6**, No. 9 (1965).
25. We thank C. A. Stone for encouraging this research and for obtaining support for this study from the in-house research committee of the IIT Research Institute. J. Woodman and F. Narin provided valuable assistance with the albedo and vapor abundance calculations. The albedo calculations employed in this paper were originally published by one of us (J.G.) in a thesis, "Ultraviolet Absorption Studies in Synthetic Atmospheres," Illinois Institute of Technology (1966). The present report is Publication No. 198, Spectroscopy Laboratory, Illinois Institute of Technology, Chicago.

19 December 1966 ■

Modified Cilia in Sensory Organs of Juvenile Stages of a Parasitic Nematode

Abstract. *Electron microscopical studies revealed the presence of dendritic nerve processes in sensory organs of the third- and fourth-stage juveniles of* Haemonchus contortus, *which contained structures resembling modified cilia. With few exceptions, the outer circle of fibers consisted of ten doublets, and in place of typical cilia-like central fibers were small microtubules or vesicles varying in number from zero to five.*

Nematodes, especially the free-living forms, have sensory organs in the form of bristles and papillae, which are thought to be tactile. In parasitic nematodes these structures are either absent (although the terminal branches of papillary nerves are retained) or are present as small protuberances or pits connected to terminal branches of the papillary nerves. The amphids, well developed in free-living nematodes but greatly reduced in parasitic forms, are thought to act as chemoreceptors. In parasitic forms the amphids may also have a secretory function (*1*).

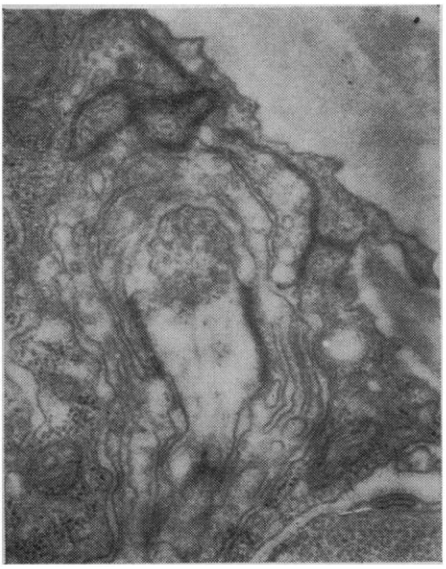

Fig. 1. Slightly oblique section of cervical papilla of third-stage juvenile showing cilia-like structure and fibers extending towards nerve axon at bottom of picture (× 31,680).

Very few details are available concerning the ultrastructure of these sensory organs. Hope (*2*) described sensory organs in *Thoracostoma californicus*, which contained structures that could be modified cilia, but he had no evidence for the presence of central fibers or basal bodies. Roggen *et al.* (*3*) described sensory organs in *Xiphenema index* as consisting, in part, of a dendritic nerve process having the structure of a cilium. The number of fibers in the cilia, however, varied (for example, 9 + 2, 9 + 4, 8 + 2, 8 + 4).

Third- and fourth-stage juveniles of *Haemonchus contortus*, after a 10- to 15-minute treatment at room temperature in $10^{-3}N$ iodine to straighten them, were fixed in Zetterqvist's fixative (*4*) for 3 hours at room temperature. It was necessary to cut each of the juveniles as short as possible to facilitate the entry of the fixative. After being washed and dehydrated each juvenile was embedded flat in Epon 812 (*5*). Each larva was then removed in a piece of Epon about 1.5 mm^3 and attached to a larger block for cutting. Sections were cut with glass knives on an LKB Ultratome, mounted on grids, and stained with Reynolds lead citrate (*6*). The sections were examined

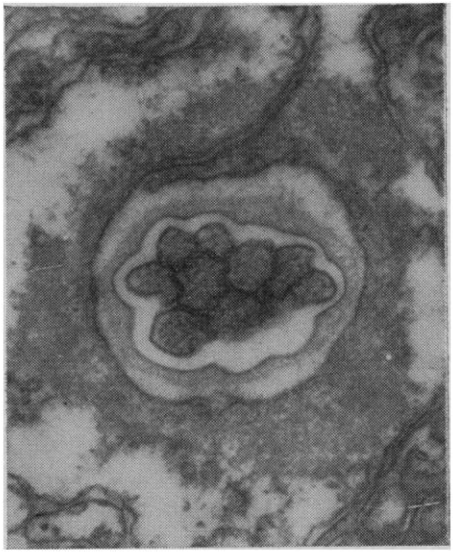

Fig. 2. Closely packed dendritic processes in the amphid near the aperture in third-stage juvenile (× 39,900).

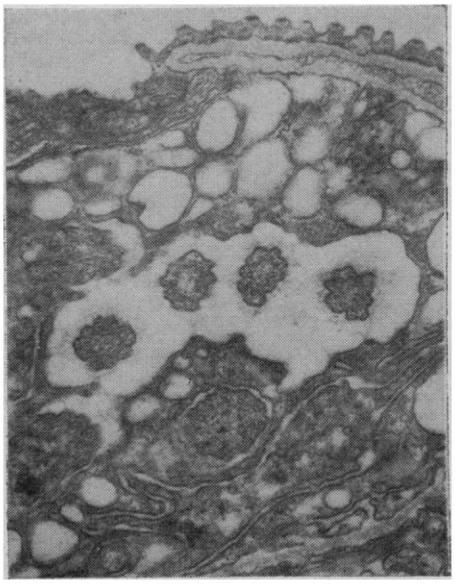

Fig. 3. Dendritic processes near the bottom of the amphid pouch showing cilia surrounded by highly vacuolated spaces. Doublet pattern clearly defined. Third-stage juvenile (× 26,040).